N O T I C E

THIS DOCUMENT HAS BEEN REPRODUCED FROM MICROFICHE. ALTHOUGH IT IS RECOGNIZED THAT CERTAIN PORTIONS ARE ILLEGIBLE, IT IS BEING RELEASED IN THE INTEREST OF MAKING AVAILABLE AS MUCH INFORMATION AS POSSIBLE

NASA

Technical Memorandum 82168

A Complete X-Ray Sample of the High Latitude (lbl > 20°) Sky from HEAO -1 A-2: Log N - Log S and Luminosity Functions

G. Piccinotti, R. F. Mushotzky, E.A. Boldt, S. S. Holt F. E. Marshall, P. J. Serlemitsos and R. A. Shafer

AUGUST 1981

National Aeronautics and
Space Administration

Goddard Space Flight Center
Greenbelt, Maryland 20771

NASA
Technical Memorandum 82168

A Complete X-Ray Sample of the High Latitude (|b| > 20°) Sky from HEAO -1 A-2: Log N - Log S and Luminosity Functions

G. Piccinotti, R. F. Mushotzky, E.A. Boldt, S. S. Holt F. E. Marshall, P. J. Serlemitsos and R. A. Shafer

AUGUST 1981

A COMPLETE X-RAY SAMPLE OF THE HIGH LATITUDE ($|b|>20^{\circ}$)

SKY FROM HEAO-1 A-2: LOG N - LOG S AND LUMINOSITY FUNCTIONS

G. Piccinotti[1], R.F. Mushotzky, E.A. Boldt, S.S. Holt,

F.E. Marshall, P.J. Serlemitsos and R.A. Shafer[2]

Laboratory for High Energy Astrophysics

NASA/Goddard Space Flight Center

Greenbelt, Maryland 20771

ABSTRACT

The HEAO-1 experiment A-2 has performed a complete X-ray survey of the 8.2 steradians of the sky at $|b| > 20^{\circ}$ down to a limiting sensitivity of $< 3.1 \times 10^{-11}$ ergs/cm^2 sec in the 2-10 keV band. Of the 85 detected sources (excluding the LMC and SMC sources) 17 have been identified with galactic objects, 61 have been identified with extragalactic objects and 7 remain unidentified. The log N - log S relation for the non-galactic objects is well fit by the Euclidean relationship. We have used the X-ray spectra of these objects to construct log N - log S in physical units. The complete sample of identified sources has been used to construct X-ray luminosity functions, using the absolute maximum likelihood method, for clusters of galaxies and active galactic nuclei.

[1]NAS/NRC Research Associate

[2]Also Dept. Physics & Astronomy, Univ. of Maryland

I. INTRODUCTION

The HEAO-1 satellite experiment A-2 (Rothschild et al. 1979) with its extended energy range, complete sky coverage, low and stable internal background and moderate spatial resolution has enabled us to create a complete catalog of X-ray sources at galactic latitudes $|b| > 20°$ down to a limiting sensitivity of 3.1×10^{-11} ergs/cm^2 sec in the 2-10 keV band. Recent identifications of these sources by modulation collimator experiments on HEAO-1 and SAS-3 as well as imaging detectors on HEAO-2 has resulted in certain identifications of all sources of flux $\gtrsim 4.0 \times 10^{-11}$ ergs/cm^2 sec, pending confirmation of two clusters and NGC 7172, and reasonable identifications for 78 out of the 85 (92%) sources in the sample. All but 9 of these identifications are extremely likely or certain. This identification ratio for the extragalactic sources compares to identification of 45 out of 67 (67%) sources in the sample of Warwick and Pye (1979).

The completeness of this sample enables construction of the number-intensity distribution (log N - log S) for X-ray sources as well as developing X-ray luminosity functions for clusters of galaxies and active galactic nuclei. In addition the body of X-ray spectral data returned by A-2 allows us to cast the log N - log S distribution in absolute rather then instrument dependent units which enables comparison with the log N - log S relation in different X-ray energy bands (cf. Giacconi et al. 1979).

Analysis of this data shows that the source counts are well fit by a "Euclidean" law with

$$\frac{dN}{dS} = 16.5 \, S^{-5/2} \, (R15 \; cts/sec)^{-1} \; sr^{-1}$$

consistent with previous results despite the quite different samples (Warwick

and Pye 1978; Schwartz 1979). The luminosity functions are well fit by power law representations with

$$\frac{dN}{dL_{44}} \overset{<}{=} 3.5 \quad 10^{-7} \ L_{44}^{-2.15} \ (10^{44} \ erg/sec)^{-1} \ Mpc^{-3}$$

for clusters of galaxies, and

$$\frac{dN}{dL_{44}} \overset{<}{=} 2.7 \times 10^{-7} \ L_{44}^{-2.75} \ (10^{44} \ erg/sec)^{-1} \ Mpc^{-3}$$

for active galactic nuclei, similar to previous results (McKee et al. 1980; Pye and Warwick 1979). Integration of the luminosity functions over the $< 10^{42.5} - 10^{45}$ erg/sec range within which they are well determined results in estimates of the contribution of clusters and active galactic nuclei to the integral 2-10 keV unresolved X-ray background of $< 4\%$ for clusters and $< 20\%$ for active galaxies. Using these luminosity functions, with no evolution, we estimate that $< 30\%$ of the sources seen in the Einstein Observatory deep survey (Giacconi et al. 1979) should be relatively low luminosity ($L < 1 \times 10^{44}$ erg/sec) nearby ($z \leq 0.5$) objects.

II. DATA ANALYSIS AND SOURCE SELECTION

The HEAO-1 A-2 experiment, described in detail by Rothschild et al. (1979), provided two independent, low background, high sensitivity surveys of the entire sky six months apart. We have analyzed the A-2 data in order to obtain a complete flux limited sample of extragalactic X-ray sources. The region between $-20°$ and $+20°$ in galactic latitude has been excluded to minimize contamination from galactic sources. A circle of 6 degrees radius around the LMC sources has been also excluded to prevent confusion problems. Therefore, we remain with 65.5% of the sky (8.23 ster). The statistical

significance of the existence of the sources is tested by determining the decrease in χ^2 when the new source is added to the model. All sources in the sample give a decrease in χ^2 of at least 30. The probability of having, by chance, a decrease of 30 in χ^2 with two degrees of freedom (scan angle and intensity) is 3×10^{-7}. This probability is almost the same as the one associated with a deviation of 5σ in a Gaussian distribution (6×10^{-7}). Therefore, we can also state that the lowest statistical significance for the existence of the sources included in our sample is 5σ, as required by the maximum likelihood methods we use to determine the log N - log S parameters (see Section IV-1). Taking into account this statistical significance requirement we estimated the completeness level of the first and the second scan as 1.25 and 1.8 R15 counts/sec respectively, see Figure 1. One R15 count/sec ≤ 2.17 erg cm^{-2} sec^{-1} in the 2-10 keV energy band for a power law spectrum with photon index 1.65. R15 is a counting rate derived using the $1.5^\circ \times 3^\circ$ FWHM fields of view of the second layer of the argon counter and both layers of a xenon counter. This combination has a FWHM for the quantum efficiency from $<$ 3 to $<$ 17 keV (Marshall et al. 1979).

The second pass is less sensitive on average, because much more time was spent in pointing at sources. We shall be more concerned with the first pass data in deriving best fit parameters and use the second pass ones mostly as an independent confirmation.

III. OBSERVATIONS

A. The Sample

Table 1 contains all the relevant data for the 68 sources either brighter than 1.25 R15 c/s in the first scan which corresponds to days 248-437 of 1977, or brighter than 1.8 in the second scan, days 73-254 of 1978. Source names are listed in column 1. Column 2 contains previous catalog names.

First pass fluxes and 1σ errors are in column 3, while the second pass ones are in column 4. Some fluxes may differ slightly from previously reported results, as different procedures have been used; e.g., in the recent paper by McKee et al. (1980) fluxes have been obtained fixing the X-ray position at the optical position, instead here we have used the best fit X-ray position to derive the flux. Available identifications are listed in column 5. The type of object is in column 6. One * in column 7 indicates firm identifications (i.e. as provided by the SAS-3 or HEAO-1 modulation collimators or by the Einstein X-ray telescope), two * indicates possible identification consistent with larger error boxes. Redshift values and references are given in column 8. Spectral information is now available for more than half of our sources (Mushotzky et al. 1980; Worrall et al. 1980; Mushotzky 1979; Holt 1980; Boldt 1980), we quote in column 9 conversion factors between R15 counts/s and ergs $cm^{-2} s^{-1}$. When spectral information is lacking we assumed a 6 keV thermal bremsstrahlung spectrum for all sources identified with clusters and a 1.65 photon index power law for all sources identified with active galaxies. An average conversion factor value of 2.5×10^{-11} ergs $cm^{-2} s^{-1}$/R15 counts s^{-1} was assumed for the few unidentified sources. Columns 10 and 11 contain the first and second pass luminosities in units of 10^{44} erg s^{-1} calculated for H_o = 50 km/s/Mpc and q_o = 0.5. Column 12 contains notes.

B.   Classes of Sources

Sixty of the 82 sources brighter than 1.25 counts s^{-1} in the first scan and not definitely associated with galactic objects have been associated with extragalactic objects. Only 7 remain unidentified at the present time. These 60 identified sources subdivide almost equally between clusters of galaxies (30) and single galaxies (30). Most of the 30 galaxies are Seyfert galaxies of class 1 or 2, but we have also 1 QSO (3C 273), 4 BL Lac objects, and 1

6

"normal" galaxy (NGC 7172). Note that M31 and the Magellanic Cloud sources are not included in our extragalatic sample because they represent a local inhomogeneity as part of the local group of galaxies. Table 2 lists the 17 high galactic latitude sources not included in our extragalactic sample because they have been identified with galactic or "local" objects. The second pass sample contains only 37 sources brighter than 1.8 R15 counts/sec, all but one identified. The source classification is consistent with the first pass. Assuming Poisson errors, clusters contribute 50 ± 9% of the identified sources in the first pass and 61 ± 13% in the second. Galaxies contribute 50 ± 9% in the first scan and 39 ± 10% in the second.

C.   New Sources and Sample Completeness

H0328+025 and H0917-075 are the only entirely new sources in Table 1. Figure 2 shows their error boxes. All the other sources in Table 1 have been listed somewhere else before. The improvement in our sample, as compared to previously reported ones, is due to a better rejection of non-extragalactic sources, made possible by the recent identifications, and to a uniform sky coverage to a relatively low limiting flux.

As the instrument has a fairly large ($1.5^\circ \times 3.0^\circ$) angular resolution the possibility of source confusion must be considered. The total area of the sky included in this survey is approximately 2.7×10^4 square degrees, therefore there are about 6×10^3 independent positions on it. As the high galactic latitude X-ray sources bright enough to give confusion problems at our sensitivity level cannot be more than a hundred using the log N-log S relation derived later (taking into account also the possibility that two weaker sources can simulate a source bright enough to be included in our list) we therefore expect negligible confusion. That is using $\frac{dN}{dS} < 16.5\ S^{-1.5}$ there are roughly 65 resolution elements per source, of S > 1.25 cts, well above the

confusion level of 25 beam areas per source often quoted in the literature. In addition the uniform sky coverage at the chosen sensitivity levels provided by this experiment and the availability of two independent sets of data for cross-checking purposes support our confidence in the completeness of our sample.

D.   Space Distribution of Sources

Since the pioneering work of DeVaucouleurs (1958) much attention has been devoted to finding evidence of a supercluster centered in the Virgo cluster of galaxies. We plotted the positions of our sources in supergalactic coordinates looking for some kind of anisotropy. Figure 3 shows the 1st pass sample. Obviously, no anisotropy is observed as most sources lie beyond the supercluster. If we restrict our attention to the 12 sources with redshifts less than .01 (in boxes in Figure 3), we see that 9 are in the center region of the supercluster while 3 are in the anticenter and that all but one have supergalactic latitude less than 30 degrees in absolute value This result, which is significant at the few percent level, suggests that close X-ray galaxies may lie preferentially in the supergalactic plane. But no conclusion can safely be made from such a small number of objects at present.

IV.   THE NUMBER-FLUX FUNCTION

The usual power law form

$$N(S) = KS^{-\alpha} \qquad (R15 \text{ counts/sec})^{-1}sr^{-1} \qquad (1)$$

has been assumed for the number-flux relation. The various methods applied to estimate the coefficient K and the differential exponent α as well as to evaluate the goodness of the fit are outlined in the next section.

A.   Statistical Methods

1. Maximum Likelihood

Crawford, Jauncey and Murdoch applied the maximum likelihood method to unbinned data in order to estimate the slope of the number-flux relation of radio sources. In the first paper (Crawford et al. (1970) a solution is worked out for error free data. In the second paper (Murdoch et al. 1973) the method is extended to include errors on the measured fluxes. Numerical corrections to the error free answers were calculated for the special case of Gaussian distributed errors. In the same paper it was pointed out that a minimum signal-to-noise ratio of five is required so that the uncertainty in the correction factor due to weaker sources does not dominate the correction itself. This is why we excluded from our sample sources with statistical significance less than 5σ. In both Papers I and II the Kolmogorov-Smirnov test (here after: K-S test) was suggested to evaluate the goodness of the fit obtained. In the remainder of this paper we will refer to this method as to the Maximum Likelihood (ML) method.

2. Absolute Maximum Likelihood

The ML method assumes the same underlying error distribution for all the souces in the sample, i.e. it assigns the same 1σ error to all the sources. As we deal with sources of greater than 5σ significance the error assumed is one fifth of the minimum flux in the sample, or .25 R15 counts s^{-1} in the first scan and .36 R15 counts s^{-1} in the second. Table 1 shows that these values are not very far from the actual errors. However Lightman et al. (1980) have developed a refinement of the ML method in connection with the K-S test capable of handling sources with their own experimental error. Following those authors we will call this new statistical method the "Absolute Maximum Likelihood" (AML) method. Lightman et al. (1980) worked out the AML method on general grounds and then applied it to the evaluation of globular cluster

X-ray source masses. As this is the first application of the AML method to the number flux function, we give a short outline of the method below. Assuming the form (1) for the number-flux relation and a Gaussian form $\rho(F_i, \sigma_i, S)$ for the error distribution of the measured fluxes we evaluated numerically the integral probabilities $\overset{<}{P}_i(\alpha)$ as

$$\overset{<}{P}_i(\alpha) = \frac{\int_{F_{min}}^{F_i} dF \int_{F_{co}}^{\infty} dS \; N(S,\alpha) \; \rho(F,\sigma_i,S)}{\int_{F_{min}}^{\infty} dF \int_{F_{co}}^{\infty} dS \; N(S,\alpha) \; \rho(F,\sigma_i,S)} \qquad (2)$$

where S is the true flux, F_i and σ_i are the measured flux and error of the i-th source. F_{co} is a cutoff value used to avoid the apparent divergence at F = 0. As in Murdoch et al. (1973) the particular choice of the cutoff value does not affect the value of the integral as long as the statistical significance of the sources is at least 5σ. F_{min} is the sensitivity limit of the sample. For every assumed α we computed the $\overset{<}{P}_i(\alpha)$ for all the sources. The $\overset{<}{P}_i(\alpha)$ should be uniformly distributed between 0 and 1. Following Lightman et al. we evaluated the maximum deviation from the uniform distribution:

$$D_{max}(\alpha) = \max_{i=1,N} [D_i(\alpha)] = \max_{i=1,N} \left(\left| \overset{<}{P}_i(\alpha) - \frac{i}{N} \right| \right) \qquad (3)$$

where N is the number of sources in the sample and the $\overset{<}{P}_i(\alpha)$ have been sorted in ascending order. Then we calculate the probability $P(D_{MAX}(\alpha))$ of observing deviations greater than $D_{MAX}(\alpha)$ from the formula for the K-S statistic given by Birnbaum and Tingey (1951). The $(\alpha, P(D_{max}(\alpha)))$ function is then plotted. The best fit value of α is the one corresponding to the maximum

value P_{MAX} of the $P(D_{max}(\alpha))$ distribution. Obviously P_{MAX} must be greater than some minimum value (say 10%) in order to accept the model. The range in α for results given below on α are evaluated from the values α_1 and α_2 of α, which reduce $P(D_{max}(\alpha))$ to $P_{MAX}/2$.

3.Chi-Square

Both the ML and the AML methods are independent of the coefficient κ of the number-flux relation, as κ is lost in normalizing the probabilities. Therefore, we used the χ^2 method to determine κ. Bins with equal expected number of sources for $\alpha = 2.5$ have been used for the χ^2 calculations. Of course, in calculating confidence bounds, we have assumed that the functional form of the distribution is the "true" one. If better data later shows that this is not true our confidence values are not applicable.

V. LOG N - LOG S RESULTS

The ML method applied to the 60 non-galactic sources brighter than 1.25 R15 counts s^{-1} in the first pass gives (in this section we use R15 counts s^{-1} as the unit)

$$\alpha = 2.67 \pm .23$$

with a goodness of fit probability (evaluated using the KS test) of 39.5 percent.

For the 37 non-galactic sources brighter than 1.8 R15 counts s^{-1} in the second pass the ML result is

$$\alpha = 2.74 \pm .32$$

with a probability of 17.5 percent.

The AML results are

$$\alpha = 2.63 \pm .2$$

in the first pass, see Figure 4a, and

$$\alpha = 2.74 \pm .22$$

in the second, see Figure 4b.

The 68 and 95 percent probability contours for the 1st pass values of κ and α evaluated with the χ^2 method are plotted in Figure 4c The χ^2 best fit values and 1σ errors for the number-flux function parameters are

$$\alpha = 2.72^{-.10}_{+.15} \qquad (4)$$

$$\kappa = 20^{-2.6}_{+4.0} \quad (R15 \ counts/sec)^{\alpha-1} \ sr^{-1}.$$

The differential number-flux data as well as the best fit function

$$N(S) = 20 \ S^{-2.72} \quad (R15 \ counts/sec)^{-1} \ sr^{-1}$$

are plotted in Figure 5; the χ^2 value of the fit is 2.79 for 6 degrees of freedom, corresponding to a probability $P(> \chi^2) \le 83\%$. The limited size of the second scan sample does not allow a good estimate of the probability but the results are consistent with the first pass ones.

C.   Number Flux Relation in Physical Units

Using the conversions factors listed in column (9) of Table 1 we can

express the fluxes in ergs cm^{-2} s^{-1} and evaluate the number-flux relation accordingly. Conversion factors range approximately from 2.0×10^{-11} to 2.9×10^{-11} ergs cm^{-2} s^{-1} (R15 counts $s^{-1})^{-1}$, the highest values referring to soft spectra sources whose emission peak lies below our instrument energy window. As a consequence of the different conversions factors the completeness level of the samples when fluxes are in ergs cm^{-2} s^{-1} is equal to the former completeness level in R15 counts s^{-1} times the maximum conversion factor: that is $< 3.6 \times 10^{-11}$ ergs cm^{-2} s^{-1} for the first pass and 5.2×10^{-11} ergs/cm^2 sec in the second pass. The 1st scan sample with this flux restriction contains 51 sources: 25 clusters, 22 "galaxies" and 4 unidentified sources. The best fit values and 1 σ errors for the number-flux function parameters obtained with the three methods agree with

$$\alpha \leq 2.85 \pm .3$$
$$\kappa \leq (5.65^{-1.3}_{+1.9}) \times 10^{-19} \ (\text{ergs} \ cm^{-2} s^{-1})^{\alpha-1} sr^{-1} \tag{5}$$

The 32 second scan sources brighter than 5.2×10^{-11} ergs cm^{-2} s^{-1} give us a best fit of slightly steeper slope $\alpha \leq 3.1 \pm .4$.

VI. DISCUSSION OF THE RESULTS

All the first pass samples, whether fluxes are expressed in R15 counts s^{-1} or in ergs cm^{-2} s^{-1} are consistent with the five halves Euclidean slope (see Figures 6 and 7). The slight preference for a steeper than Eucledian slope is due to the distribution of the brightest few sources in calculating the likelihood functions. It is these sources that are most sensitive to changes in α by virtue of the relatively small statistical error in their measured intensity. Our Euclidean best fit for the 1st pass data is

$$N(S) = 16.5^{+3}_{-2} \ S^{-2.5} \ (R15 \ counts/s)^{-1} sr^{-1}$$

with a χ^2 of 5.5 for 7 degrees of freedom; $\rho(\chi^2 > 5.5) \lesssim 60\%$. The AML probability for $\alpha = 2.5$ is 42.4%. Assuming an average conversion factor of 2.4 $\times 10^{-11}$ ergs $cm^{-2}s^{-1}$ (R15 counts s)$^{-1}$ the relation (4) becomes

$$N(S) \lesssim (1.9^{+.35}_{-.25}) \times 10^{-15} \ S^{-2.5} \ (ergs \ cm^{-2} s^{-1})^{-1} \ sr^{-1}$$

in agreement with the exact result

$$N(S) \lesssim (2.2^{+.3}_{-.2}) \times 10^{-15} \ S^{-2.5} \ (ergs \ cm^{-2} s^{-1})^{-1} \ sr^{-1}$$

obtained from the 1st pass complete sample for fluxes in ergs $cm^{-2}s^{-1}$ and using the conversion factors in Table 1.

VII. COMPARISON WITH PREVIOUS EXPERIMENTS

Both the Uhuru (Schwartz 1979) and Ariel 5 data (Warwick and Pye 1978) gave a flux-number function consistent with the Euclidean model. Their best fit values for the coefficient κ with $\alpha = 2.5$ and S in R15 counts s^{-1} are respectively

$\kappa = 16.5 \pm 3.9$ using 1 Uhuru ct/s = 1.0 R15 ct/sec

and

$\kappa = 15.8 \pm 4.2$ using 1 Ariel-5 ct/sec = 2.12 R15 ct/sec

in agreement with our results at the 1σ level. These conversion factors assume a mean R15 conversion factor of 2.4 $\times 10^{-11}$ ergs/sec, 1 Uhuru ct/sec = 2.4 $\times 10^{-11}$ erg/sec, and 1 Ariel-5 count/sec = 5.1 $\times 10^{-11}$ erg/sec. If we use the calibration of Marshall et al. (1979) appropriate for the active galaxies of 1 R15 ct/sec = 2.17 $\times 10^{-11}$ erg/cm^2 sec, we find $\kappa_{Uhuru} \lesssim 20$ and

$K_{Ariel-5}$ ≤ 19. The best fit slope of Warwick and Pye of 2.7 ± .2 is also consistent with our result.

VIII. LUMINOSITY FUNCTION

A. Method and Data Base

Many authors (Schwartz 1978; McHardy 1978; McKee et al. 1980; Elvis et al. 1977; Pye and Warwick 1979; Tananbaum et al. 1978; Boldt 1980) have recently considered the problem of evaluating the X-ray luminosity functions for different classes of sources principally, clusters of galaxies and active galaxies. All of them with the exception of Pye and Warwick had to rely upon optical data to select complete samples. We present here X-ray luminosity functions evaluated from X-ray flux limited samples. As we remain with a few unidentified sources, our results have some uncertainty, but we believe that the residual incompleteness should not be very important.

1. The Samples

The first pass sample of clusters of galaxies contains 30 objects. The second pass one includes 22 sources. Thirty "galaxies" are observed in the first pass, but we exclude from our sample the QSO 3C273, the 4 BL Lac objects, the peculiar galaxy M82 and the "normal" galaxy NGC 7172 as they are not homogeneous with the bulk of the sample which consists of Seyfert galaxies. Therefore we remain with 23 active galactic nuclei. The second pass sample contains only 12 objects (after excluding 3C 273 and PKS 2155-304).

The completeness of the sample is checked using the Schmidt $\langle V/V_M \rangle$ test and with a K-S test on the distribution of the V_i/V_{M_i} as suggested by Avni and Bahcall (1980). The results are listed in Table 3.

TABLE 3

| | | # OBJECTS | | K-S TEST |
CLASS OF OBJECTS	SCAN #	IN SAMPLE	$\langle V/V_M \rangle$	P(>d) %
Clusters of Galaxies	1	30	.471±.054	18.1
Clusters of Galaxies	2	22	.552±.062	11.8
Active Galaxies	1	24	.523±.059	50.4
Active Galaxies	2	12	.557±.083	56.8

The 1σ error quoted for $\langle V/V_M \rangle$ is the formal error $1/\sqrt{12N}$, where N is the number of objects in the sample (see Avni and Bahcall). All the 4 samples meet the requirements of the tests. However, we expect a small degree of incompleteness due to the unidentified sources.

2.   Methods of Analysis

Of the three methods outlines in Sec (IV-A) only the AML is suited for the determination of the luminosity function parameters. The relatively small sizes of the samples do not allow an efficient use of the χ^2 square method or of any other binned method. Moreover the ML method in the form developed by Crawford, Jauncy and Murdoch cannot be used because of its assumptions of a single underlying error distribution. This last hypothesis was reasonably satisfied by the flux data in the evaluation of the log N log S parameters, as we already pointed out, but is not satisfied at all by the luminosity data, as the errors are proportional to the square of the redshift of the sources:

$$\sigma_{L_i} \approx z_i^2 \, \sigma_{F_i} \tag{6}$$

On the contrary the AML method is well suited for the task. The description of Section IV-A still applies. However, instead of calculating the probabilities of eq (2) we evaluated the probabilities:

$$\overset{<}{P}_i(q) = \frac{\int_0^{L_i} dL' \; L_{min} \int^{L_{max}} d\overline{r} \; f(L,q) \; V_{max} \; (L,F_{min}) \; \rho(L,\sigma_L, L_i)}{\int_0^{\infty} dL' \int_{L_{min}}^{L_{max}} dL \; f(L,q) \; V_{max} \; (L,F_{min}) \; \rho(L,\sigma_{L_i}, L')} \qquad (7)$$

Eq. (7) gives the integral normalized probabilities of observing a source with measured luminosity less or equal to L_i, assuming a Gaussian error distribution with standard deviation σ_{L_i}, and for the differential luminosity function the form $f(L,q)$ where L is the true luminosity and q represents the functional parameters to be determined. L_{min} and L_{max} are the lower and upper boundaries of the luminosity function. V_{MAX} is the maximum volume at which one could detect the source and depends on the sensitivity limit of the sample. For a source of luminosity L in a sample of minimum sensitivity F_{MIN} the maximum visibility volume V_{MAX} is proportional to

$(\sqrt{L/F_{min}})^3$ Note that Eq. (7) does not take in account errors on the redshift z. The AML method can determine the form of the luminosity function but not its absolute value. Therefore we have used a least squares fit to the unbinned data to evaluate the multiplicative coefficient.

B.   Results

1.   Clusters of Galaxies Luminosity Function

We considered two different forms for the luminosity function: the power law form

$$f(L) = KL^{-\gamma}$$

and the exponential form

$$f(L) = Ke^{-L/L_o}$$

between the minimum (L_{44min}) and maximum (L_{44max}) observed luminosities, expressed in units of 10^{44} ergs sec^{-1}. The normalization for a power law luminosity function scales as H_o^{-1}.

Clusters of Galaxies

Figure 9 represents the AML probabilities for the slope of the cluster of galaxies power law luminosity function. The 1st pass best fit values for the power law parameters are

$$\gamma = 2.15^{+.12}_{-.17}$$
$$K = (3.5 \pm 1.1) \times 10^{-7} \quad (10^{44} \text{ erg/s})^{\gamma-1} \text{ Mpc}^{-3}.$$

K has been evaluated with the least squares method. The error on K has been determined by letting γ assume the 1σ extreme values of 2.03 and 2.32. Figure 8a gives a binned representation of the data with the best fit luminosity function. Each bin contains three sources, except for the highest luminosity bin which contains five. The second pass results are

$$\gamma = 2.13^{+.16}_{-.24}$$
$$K = (3.8 \pm 2) \times 10^{-7} \quad (10^{44} \text{ ergs/s})^{\gamma-1} \text{ Mpc}^{-3}$$

Figure 8b give the binned representation. The minimum luminosity object in both the 1st and the 2nd pass at 2.4×10^{43} (ergs/s) is the Virgo cluster. The highest luminosity cluster is Abell 2142 with 2.8×10^{45} (ergs/s).

The exponential form of the luminosity function has also been considered, but the quality of the fit is poorer, see Figure 10.

As the Virgo Cluster of galaxies has a "local" character, we evaluated the cluster of galaxies luminosity function without the Virgo cluster. The 1st pass sample is reduced to 29 sources, the mean V/V_{MAX} is 0.486 ± 0.055 and the K-S text on the uniformity of the V/V_{MAX} distribution gives a probability of 24.7%. The 2nd pass sample contains 21 sources, the mean V/V_{MAX} is 0.576 ± .063 and the K-S probability is 6.1%. Figure 9 gives the usual $(\gamma, P(\gamma))$ probability curves for the power law slope. The best fit values for the parameters are

1st scan $\gamma = 2.03 \pm .18$
$$K = (2^{+1.2}_{-.8}) \times 10^{-7} \quad (10^{44} \text{ ergs/s})^{\gamma-1} \text{ Mpc}^{-3}$$

2nd scan $\gamma = 2.07^{+.2}_{-.25}$
$$K = (3.2 \pm 2) \times 10^{-7} \quad (10^{44} \text{ ergs/s})^{\gamma-1} \text{ Mpc}^{-3}.$$

The minimum luminosity is now $\leq 3.6 \times 10^{43}$ ergs/s (Abell 1060) in both first and second scan. The exponential fit is again poorer, see Figure 10.

2.   Active Galaxies

   i.   Luminosity Function

      The insert in Figure 11 represents the AML probability for the power law slope of the active galaxies differential luminosity function calculated from the 1st pass data. The best fit values for the power law parameters are:

$\gamma = 2.75 \pm .15$
$$K = (2.7 \pm .15) \times 10^{-7} \quad (10^{44} \text{ ergs/s})^{\gamma-1} \text{Mpc}^{-3}$$

NGC 3227 is the weakest source in the sample with 1.75×10^{42} ergs/s and

IIIZw2 is the brightest with 1.3 x 10^{45} ergs/s. Figure 11 shows the binned representation (3 sources/bin). This result is similar to that of Boldt (1980) and Pye and Warwick (1979). The exponential form for the luminosity function is not acceptable as the probabilities are always less than 2%.

The second pass sample is too small for a good determination of the luminosity function, however we find power law slopes steeper but consistent with the first pass ones

ii. A Lower Limit to the Active Galaxy Luminosity Function

The active galaxies contribution to the cosmic X-ray background depends strongly on the lower luminosity limit of the luminosity function. The lower luminosity limit for which the function can represent the data, L_{44MIN}, can be calculated by noting that the luminosity function must be consistent with the log N - log S observations. Namely, we can set a lower limit on L_{44MIN} by requiring that the number of active galaxies brighter than 1.25 R15 counts/sec expected from the luminosity function does not exceed the observed number plus 1 or 2 times the square root of the expected number.

From eq (14.7.35) of Weinberg (1972), and assuming a power law luminosity function we have (for $\gamma \neq 2.5$ and $\gamma \neq 3$)

$$N(>S) \simeq KA \left[\frac{1}{2.5-\gamma} [L^{2.5-\gamma}]_{L_{MIN}}^{L_{MAX}} S^{-3/2} - \frac{B}{3-\gamma} [L^{3-\gamma}]_{L_{MIN}}^{L_{MAX}} S^{-2}\right] \qquad (8)$$

where: S is the flux in ergs cm^{-2}s^{-1}

K and γ are the parameters of the differential power law luminosity function in Mpc^{-3} (erg/sec)$^{-(\gamma-1)}$

L_{MAX} and L_{MIN} are the upper and lower limit of the luminosity function (actually N(>S) depends strongly on L_{MIN} and very weakly on L_{MAX})

all the luminosities are in ergs/s

$A = 3.20 \times 10^{-75}$

$B = 4.7 \times 10^{-29}$ (assuming $H_0 = 50$ km/s/Mpc)

N(>S) is the total number of sources in the sky uncorrected for sky coverage. The second term of this equataion represents a first order cosmological correction to the Eucledian result.[1]

....

(1) Footnote:

For L in units of 10^{44} erg/sec equation (8) has constants

$A = 3.2 \times 10^{-9}$

$B = 2.3 \times 10^{-7}$ $(H_0/50)$ $(1+\Gamma)$ where Γ is the spectral index of the source (here chosen to be .7)

....

Assuming an average conversion factor of 2.17×10^{-11} ergs $cm^{-2}s^{-1}$ per R15 counts s^{-1} we find that the 1σ lower limit on L_{MIN} is 4×10^{42} when γ is 2.75 and K is 2.68×10^{-7} $(10^{44}$ ergs/s$)^{-1}$ Mpc^{-3} and L_{MAX} varies between 5 and 15 x 10^{44} ergs/sec.

In Table 4 we show the 1 and 2σ limits on L_{MIN} as a function of L_{MAX} and γ. We note that we have not included in Table 4 the possibility that all (or some) of the unidentified sources could be Seyfert galaxies. However, considering the distribution of identified sources with flux < 3 R15 cts/sec, we would expect, at most, 3 of these unidentified objects to be active galaxies.

TABLE 4

APPROXIMATE L_{MIN} FOR VALUES OF L_{MAX} AND γ

$L_{MAX} = 1.5 \times 10^{45}$ $L_{MAX} = 3 \times 10^{45}$

	γ				γ	
	2.6	2.75	2.9	2.6	2.75	2.9
1σ	1.5×10^{42}	2.5×10^{42}	4.5×10^{42}	1.5×10^{42}	3.0×10^{42}	4.5×10^{42}
2σ	4.5×10^{41}	1.5×10^{42}	2.5×10^{42}	5.5×10^{41}	1.5×10^{42}	3.0×10^{42}

C.   Discussion

1.   Clusters of Galaxies

We note that our luminosity function for clusters of galaxies is very similar to the result of McKee et al. (1980). This indicates that, whatever selection effects are operating in making a X-ray or optically complete sample, they do not strongly bias the result. However there is a strong overlap in the individual objects between this sample and McKee's. The method we have used has allowed us in principle to discriminate between exponential and power law luminosity functions for clusters. It is somewhat surprising that a power law is favored, since it requires a change in form at low luminosities in order not to exceed the space density of all clusters (Bahcall 1979). However, the contribution of clusters to the diffuse X-ray background (DXRB) depends only weakly on the lower limit chosen. We do remind the reader that an exponential form is _not_ excluded. Our data are not capable of rejecting the exponential form. They are also not capable of determining well the three constants in Bahcall's (1979) suggested form of the luminosity function.

Keeping in mind that the mean X-ray spectrum of clusters differs significantly from the diffuse X-ray background we shall, for historical reasons, compare the 2-10 keV volume emissivity of clusters to that of the diffuse X-ray background. For $q_o = 1/2$, $H_o = 50$ km/sec/Mpc the 2-10 keV background has a volume emissivity of $\lesssim 2.4 \times 10^{39}$ erg/sec/Mpc^3. The

contribution of clusters is

$$\int_{L_{MAX}}^{L_{MIN}} f(L) \ LdL \ \overset{<}{\sim} \ 1 \ x \ 10^{38} \ ergs/sec/Mpc^3$$

(for $L_{MAX} = 3 \ x \ 10^{45}$ ergs/sec, $L_{MIN} = 1 \ x \ 10^{43}$ ergs/sec, where we have used the 1st pass cluster power law luminosity function without the Virgo cluster). Therefore, in an average sense, clusters contribute $<$ 4% of the 2-10 keV background. (For a more accurate treatment of the problem which includes the effect of the spectral differences of clusters from the background see McKee et al. 1980 and Marshall et al. 1980). We note that the present value agrees well with the estimate made by Marshall et al. (1980) of the maximum possible contribution of clusters if they were not to distort the thermal bremsstrahlung fit to the spectrum of the DXRB in the 3-50 keV band. We note that the relatively soft spectra of clusters should result in an increase in their contribution to the DXRB in the Einstein Observatory energy range.

2. Active Galaxies

The luminosity function derived here is in reasonable agreement with those derived previously by Pye and Warwick (1979) and Boldt (1980) in both slope and normalization. Using a lower bound of $3.0 \ x \ 10^{42}$ ergs/sec and a upper bound of $1.5 \ x \ 10^{45}$ erg/sec for our luminosity function results in a volume emissivity of $<$ $4.9 \ x \ 10^{38}$ ergs/sec Mpc^3 or a contribution of $<$ 20% to the 2-10 keV DXRB. If the lower limit is $1.2 \ x \ 10^{42}$ (see Table 4) the contribution to the DXRB is $<$ 40%. In fact, in order not to exceed the DXRB the luminosity function of AGN's must flatten at $L \ \overset{>}{\sim} \ 3 \ x \ 10^{41}$ ergs/sec (De Zotti 1980). There is a strong indication of such a flattening in the optical luminosity function (Huchra and Sargent 1973; Huchra 1977; Huchra 1980) at

$M_v < -21.5$ ($H_o = 50$) equivalent to a optical bolometric luminosity of $< 1.2 \times 10^{44}$ ergs/sec. Since the slope of the optical luminosity function, at higher luminosities, is the same, within errors, (Huchra and Sargent 1973; Weedman 1979) as the X-ray function it is tempting to associate the bend in the optical luminosity function with the bend in the X-ray function and therefore derive a $L_{opt}/L_x < 35$. This value is rather larger than that found by examing individual objects (Kriss et al. 1980; Elvis et al 1978). This may be due to the fact that most of the optical flux from low luminosity active galaxies does not come from the nucleus but from the stellar population.

The total space density of X-ray emitting active galaxies in the luminosity range $3 \times 10^{42} - 1.5 \times 10^{45}$ is $< 7 \times 10^{-5}$ Mpc^{-3} which is $< 1.5\%$ of all galaxies of $M_p < -19$ (Huchra 1977). This compares to a space density of active galaxies of $M_p < -19$ of $< 5 \times 10^{-5}$ Mpc^{-3} (Huchra 1977, 1980). It thus seems, to first order, that all active galaxies of $M_p < -19$ emit X-rays at $L_x > 3 \times 10^{42}$ ergs/sec. For a flat universe there are (assuming no evolution) $< 4 \times 10^7$ X-ray emitting active galaxies with $L_x > 3 \times 10^{42}$ with $z \lesssim 3.5$.

We can also estimate, the number of sources per square degree expected in the Einstein deep survey if the luminosity function used in this paper does not evolve strongly in either slope or norm and that spectral effects, such as low energy absorption, are not important. With $q_o = .5$, $L_{min} = 3 \times 10^{42}$ in the 2-10 keV band and, $S_{min} = 5 \times 10^{-14}$ ergs/cm^{2}sec in the 2-10 keV band, (which corresponds to the Einstein "deep survey" limit for a $\alpha = 0.7$ source we predict < 6 active galaxies per square degree and < 1.3 clusters per square degree, compared to the 19 ± 8 total sources per square degree seen by the Einstein Observatory (Giacconi et al. 1979). DeZotti (1980) has performed a similar calculation and finds < 5 active galaxies per square degree for $L_{min} =$

9.1×10^{41} and $L_{max} = 2.9 \times 10^{44}$ ergs/sec in the 2-6 keV band and assuming that the slope of the luminosity function is 2.5. Since most of the objects are near L_{min} we would expect many of the Einstein survey objects to be Seyfert galaxies of $L_x \lesssim 5 \times 10^{42}$ erg/sec and $z \lesssim .20$. This is a consequence of the well known fact that if the luminosity function is steeper than 2.5, and barring strong evolution, when one looks at fainter objects one is looking primarily lower in the luminosity function rather than at higher redshift objects.

A simple way to look at the problem is to examine the number of objects predicted by our best fit luminosity function which would have redshifts (z) $\lesssim 0.5$ and would have luminosities high enough to have been included in the Einstein Deep Survey. (We shall use $q_0 = .5$ or 0 geometry for simplicity). For $S_{min} = 5 \times 10^{-14}$ ergs/cm^2 sec in the 2-10 keV band and $q_0 = .5$ that we predict $< 1.4 \times 10^4$ sources/ster due to active galaxies and $< 1.4 \times 10^3$ sources/ster due to clusters compared to the $6.3 \pm 2.6 \times 10^4$ sources/ster seen in the deep survey (Giacconi et al. 1979). We therefore predict that $< 25 \overset{+17}{\underset{-8}{}}$

of the sources in the deep survey are low (L $\lesssim 4 \times 10^{43}$) close by (z $\lesssim .5$) active galaxies or clusters of galaxies of luminosity $> 1 \times 10^{43}$ erg/sec. That this was a likely situation was noted by Fabian and Rees (1978). (If $q_0 = 0$ the number of sources increases to $< 2.1 \times 10^4$ sources/ster and the calculated contribution to the Einstein source counts to 35^{+24}_{-11}%).

Both the contribution of active galaxies to the DXRB and their contribution to the Einstein source counts depend sensitively on the lower limit, L_{min}, of the luminosity function used. It is possible that the luminosity where the flattening of the luminosity function takes place could be higher than our calcuated value if we allow a two slope model of the luminosity function rather than our simple single slope power law model with a

cutoff. However our data are not good enough to constrain such a model. We therefore _strongly_ caution the reader that these results are _model dependant_ and should be treated as such.

IX. CONCLUSIONS

We have performed an all sky survey of X-ray sources complete to a limiting sensitivity of 3.1×10^{-11} ergs/cm^2 sec in the 2-10 keV band. Of the 85 detected sources only 7 remain without reasonable identifications. The log N- log S relation for extragalactic sources is well fit by a Euclidean law $\frac{dN}{dS} = 16.5 \ S^{-2.5}$ where S is in R15 ct/sec or $\frac{dN}{dS} = 2.2 \times 10^{-15} \ S^{-2.5} \ (erg/cm^2 s)^{-1} \ sr^{-1}$ where S is in erg/cm^{2}s in the 2-10 keV band. This complete sample has allowed construction of luminosity functions based on a flux limited sample for clusters of galaxies and active galactic nuclei. These functions are well represented by power laws of slope 2.05 and 2.75 respectively. The sample enables us to estimate that the luminosity function for active galaxies should flatten at L $\lesssim 3 \times 10^{42}$ erg/sec in the 2-10 keV band. The space density of X-ray emitting active galaxies is approximately the same as that of optically selected Seyfert galaxies.

Integration of the best fit luminosity functions indicates that clusters of galaxies contribute $\lesssim 4\%$ of the 2-10 keV diffuse X-ray background and active galactic nuclei $\lesssim 20\%$. The sum of these contributions is very similar to the 26±11% contribution due to resolved due to sources seen in the Einstein deep survey. We also predict that many of the objects seen in the deep survey should be local, (z < 0.5), relatively low luminosity active galactic nuclei and clusters of galaxies. In order to determine more accurately the contribution of low luminosity active galaxies to the diffuse X-ray background one would have to sample the luminosity range $10^{41-42.5}$ over large solid angles. This would require a complete sky survey with $\lesssim 30$ times the

sensitivity of the present one and a angular resolution $\lesssim$ 20 times better. Such a survey would also extend the luminosity function up to luminosities of $\lesssim 10^{47}$ ergs/sec. We stress the importance of a complete unbiased X-ray survey with good identifications in determining log N - log S and luminosity functions since there are various classes of sources of widely varying X-ray to optical luminosities. We feel that this strategy rather then deep observations over small solid angles will determine log N - log S and the luminosity functions most accurately for the local epoch since for a given observing time and fixed instrumental parameters the number of observed sources greater than some statistical limit is maximized when the solid angle is maximized at a given completeness level for a photon limited experiment.

TABLE 1

(1)	(2)	(3)	(4)	(5)	(6)	(7)	(8)	(9)	(10)	(11)	(12)
H0008+105	2S0007+107	1.64 .21	<1.35	IIIZW2	1	*	.0098 W3	2.175	12.9	0.82	
H0039-096	2A0039-096 4U0037-10	2.64 .24	3.21 .38	ABELL 85	6	*	.0499 HSM	2.500	7.25	4.76	
H0054-015	2A0054-015 4U0050-01	1.74 .33	2.13 .35	ABELL 119	6	*	.0446 N	2.550	3.89		
H0111-149		1.49 .22	.93 .35		7			2.500			1
H0122-591	2A0120-591 4U0106-59	1.29 .18	1.38 .2	FAIRALL9	1	*	.0461 W3	2.175	2.63	2.01	
H0123-352	2A0120-353 4U0115-36	2.52 .19	1.04 .28	NGC525A	1	*	.018 W3	2.175	.772	.319	
H0206-019	H0206-019	1.34 .23	.87 .41	MKN590	1	*	.027 V1	2.175	0.91	0.59	
H0235-52	2A0235-52	2.12 .14	.99 .23			7					
H0256+134	2A0255+132 1M0254+132 4U0254+13	2.95 .24	3.03 .33	ABELL 401	6	*	.0748 H	2.480	18.3	18.8	
H0316-443	2A0316-443 4U0321-45	1.82 .19	1.67 .23	PKS0316-443	6	**	.09 MA	2.520	16.7	9.02	
H0335+096	2A0335+096 4U0344+11	1.14 .22	1.86 .25	0335+096	6	*	.04 SC	2.810	2.25	3.67	
H0342-538	2A0343-536 1M0328-524 4U0335-54	1.4 .16	1.42 .17	CA0342-538	6	*	.052 MO	2.520	4.21	4.27	
H0411+104	2A0411+103 1M0405+100 4U0410+10	2.61 .3	2.66 .34	ABELL 478	6	*	.09 B	2.480	23.6	24.0	
H0430-616	2A0430-615 1M0426-635 4U0427-61	2.53 .11	2.88 .14	SERSIC40/6	6	*	.0601 V	2.480	10.1	11.4	
H0431-134	2A0431-136 4U0431-12	2.16 .29	1.73 .3	ABELL 496	6	*	.036 C2	2.520	3.09	2.40	
H0430+053	2S0430+05 4U0432+05	2.04 .25	1.53 .36	3C120	1	*	.033 DV	2.175	2.12	1.59	
H0548-322	1M0545-322 4U0543-31	1.7 .18	1.2 .25	PKS0548-322	3	*	.069 FD	2.675	9.64	6.80	
H0557-385	4U0557-38	1.36 .16	2.26 .21		1	*	.0334 MP	2.17500	1.62	2.70	

H0630-541	2A0626-541 4U0627-54	1.98	.13	2.23	.13	SC0630-541	6	*	.0502 V	2.520	5.55	6.25	2
H0906-095	2A0906-095 4U0905-09	3.96	.28	4.16	.26	ABELL 754	6	*	.0537 CI	2.440	12.3	12.9	
H0917-074		1.36	.28	1.21	.3		7			2.500			
H0943-141	2A0943-140 4U0937-12	3.14	.25	3.97	.54	NGC2992	2	*	.0062 DV	2.175	.114	.143	
H0952+699	2A0954+700 1M0943+712 4U0954+70	1.32	.2	1.17	.2	M82	2	*	.0013 DV	2.480	.0024	.0021	
H1019+203	A1021+198	1.71	.24	.96	.3	NGC3227	2	*	.0033 VI	2.175	.0175	.0098	
H1034-273	2A1033-270 4U1033-26	2.19	.21	2.25	.3	ABELL 1060	6	*	.0114 H	2.880	.355	.365	
H1136-375	2A1135-373 4U1136-37	1.95	.23	<.6		NGC3783	1	*	.0091 VI	2.175	.152		
H1208+397	2A1207+397 1M1207+397 4U1206+39	6.34	.26	15.64	.36	NGC4151	1	*	.0033 VI	2.070	.0607	.104	
H1219+305	2A1219+305	1.61	.25	1.3	.3	1219+305	3	*		2.340			
H1226+023	2A1225+022 4U1226+02	3.46	.26	3.8	.37	3C273	5	*	.158 MS	2.040	81.6	89.6	
H1228+127	2A1228+125 1M1228+127 4U1228+12	14.2	.33	14.25	.33	VIRGO CL.	6	*	.0037 DV	2.850	.239	.240	
H1238-049	4U1240-05	1.71	.26	1.09	.41	NGC4593	1	*	.0085 DV	2.175	.116	.0741	
H1246-410	2A1246-410 1M1247-410 4U1246-41	5.15	.23	5.64	.37	CEN CL.	6	*	.0118 FO	2.740	.851	.932	
H1256-171		1.45	.28	<1.8		ABELL 1644	6	*	.0449 HSM	2.520	3.24		
H1257-042		1.47	.27	1.41	.53	ABELL 1651	6	**	.0826 HSM	2.520	11.3	16.9	
H1257+283	2A1257+283 1M1257+281 4U1257+28	14.67	.28	16.1	.32	ABELL 1656	6	*	.023 N	2.440	8.25	9.05	
H1324-311	2A1326-311 1M1329-314 4U1325-31	2.83	.25	2.74	.45	SC1325-31	6	*	.073 L	2.520	17.0	16.4	3
H1325-028		1.47	.25	<1.0			7			2.500			
H1332-336	2S1333-34	2.12	.18	2.59	.35	MCG6-30-15	1	*	.006 V3	2.175	.0717	.0076	
H1344-333 ?	2A1344-325	3.23	.27	2.49	.37	SC1344-32	6	**	.0144 L	2.520	.732	.565	

HEAO	Alternate names					ID	N	flag	col	code	col	col	col
H1347+268	2A1346+266 4U1340+25	2.36	.25	2.91	.4	ABELL 1795	6	*	.0621	H	2.520	10.2	12.6
H1346-300	2A1347-300	3.7	.21	3.43	.37	IC4329A	1	*	.0138	VI	2.175	.665	.616
H1411-031	2A1410-029 1M1410-030 4U1410-03	2.69	.22	2.62	.43	NGC5506	2	*	.0056	DV	2.175	.0793	.0772
H1416+256	2A1415+255 4U1415+25	2.92	.23	2.77	.32	NGC5548	1	*	.0166	VI	2.175	.760	.721
H1500+060	2A1500+062 1M1514+068	3.00	.29	2.35	.36	ABELL 2029	6	*	.0767	F	2.520	19.9	15.6
H1513+070 CONFUSED? WITH 2A1519+082		1.51	.28	1.9	.36	ABELL 2052	6	*	.0344	M	2.520	1.97	2.40
H1521+282	2A1518+274 4U1521+28	1.25	.2	1.69	.33	ABELL 2065	6	*	.0721	S	2.520	7.30	9.07
H1556+274	2A1556+274 4U1556+27	3.14	.24	2.87	.23	ABELL 2142	6	*	.0963	H	2.420	27.9	25.5
H1600+161	2A1600+164 4U1601+15	1.82	.23	2.	.41	ABELL 2147	6	*	.0377	K	2.740	3.31	3.42
H1627+396	2A1626+396 4U1627+39	2.72	.18	2.82	.24	ABELL 2199	6	*	.0312	M	2.740	3.17	3.29
H1630+057	2A1630+057 4U1636+05	1.26	.24	<1.8			7				2.500		
H1652+398	4U1651+39	1.81	.18	1.71	.28	MKN501	3	**	.034	DV	2.340	2.14	2.03
H1707+788	2A1705+786 1M1706+785 4U1707+78	2.53	.12	2.42	.1	ABELL 2256	6	*	.0603	F	2.480	10.1	9.58
H1829-591	4U1830-60	1.55	.21	.71	.24		7				2.500		
H1834-653		1.36	.18	1.00	.23	ESO103-G35	1	**	.013	V3	2.175	.217	.172
H1846-786	1M1849-781 4U1916-79	1.33	.16	1.48	.21		7				2.500		
H1917-587	2A1914-589 4U1924-59	1.70	.17	1.64	.26	ESO141-G55	1	*	.0368	V2	2.175	2.29	2.12
H2009-569	2A2009-569	3.19	.21	3.09	.25	SC2008-569	6	*	.06	B2	2.520	12.0	12.4
H2041-109	2A2040-115	2.00	.24	2.41	.31	MKN509	1	*	.0355	VI	2.175	2.50	2.73
H2154-304	2A2151-316	4.30	.24	2.33	.32	PKS2155-304	3	*	.17	CTB	2.525	146.	79.1

H NAME	PREVIOUS NAMES	1ST SCAN FLUX	±ERR	2ND SCAN FLUX	±ERR	IDENTIFICATION	TYPE	QUALITY	REDSHIFT	REF			
H2151-605	2A2155-609 1M2140-602 4U2126-60	1.29	.21	1.35	.25	STR2159-602	6	**	.1000	VF	2.520	14.9	15.6
H2158-321	2A2151-316	2.00	.23	1.4	.29	NGC7172	4	**	.009	DV	2.570	.100	.126
H2209-471		1.07	.21	1.03	.28	NGC7213	1	*	.0058	DV	2.175	.0330	.0570
H2215-027	2A2220-022	1.55	.24	.98	.29	3C445	2	**	.0562	OKP	2.175	4.71	2.90
H2233-261	2A2237-256	1.39	.22	1.94	.3	NGC7314	2	**	.0056	DV	2.175	.0410	.0572
H2301-006	2A2259-005 4U2305-08	1.77	.25	1.45	.39	NGC7469	1	*	.0167	VI	2.175	.466	.302
H2302-090	2A2302-088 4U2305-07	1.88	.25	2.3	.34	MCG2-58-22	1	*	.0479	VZ	2.175	4.14	5.06
H2316-426	2A2315-428	2.51	.23	3.04	.29	NGC7582	2	*	.0048	DV	2.175	.0543	.0650
H2342+089	4U2344+08	1.31	.27	.93	.33	ABELL2657	6	*	.0414	N	2.520	2.49	1.77

COLUMN CAPTIONS:

(1) : H NAME

(2) : PREVIOUS NAMES

(3) : 1ST SCAN FLUX AND 1-SIGMA ERROR (R15 COUNTS/SEC)

(4) : 2ND SCAN FLUX AND 1-SIGMA ERROR (R15 COUNTS/SEC)

(5) : IDENTIFICATION

(6) : TYPE OF OBJECT:
1 = SEYFERT 1 GALAXY
2 = SEYFERT 2, NELG, N OR OTHER ACTIVE GALAXY
3 = BL LACERTE OBJECT
4 = NORMAL GALAXY
5 = QSO
6 = CLUSTER OF GALAXIES
7 = UNIDENTIFIED

(7) : QUALITY OF IDENTIFICATION: * = CERTAIN: SAS-3 OR HEAO-1 MODULATION COLLIMATOR POSITION OR EINSTEIN OBSERVATORY POSITION
** = POSSIBLE

(8) : REDSHIFT VALUE AND REFERENCE:
B = BAHCALL,N.A.,SARGENT,W.L.W.,1977,AP.J.,217,L19
B2 = BAHCALL,N.A.,AP.J.,217,L77
C1 = CORVIN,H.G.JR.,1971,PUBL.ASTRON.SOC.PACIFIC,83,329
C2 = CORVIN,H.G.JR.,1974,A.J.,79,1356
CMR = CANIZARES,C.R.,MCCLINTOCK,J.E.,RICKER,G.R.,1978,AP.J.,226,L1
CTB = CHARLES,P.,THORSTENSEN,J.,BOWYER,S.,1979,NATURE,281,285
DV =DEVAUCOULEURS,DEVAUCOULEURS AND CORWIN SECOND REFERENCE CATALOG OF BRIGHT GALAXIES 1976
F = FABER,S.,DRESSLER,A.,1977,A.J.,82,167
FD = FOSBURY,R.A.E.,DISNEY,M.J.,1976,AP.J.,207,L75
FO = FORMAN,W.,JONES,C.,TANANBAUM,H.,1976,AP.J.,206,L29
H = HINTZEN,P.,SCOTT,J.S.,1979,AP.J.,232,L145

HSM = HINTZEN,P.,SCOTT,J.S.,MCKEE,J.D. 1980 AP.J. IN PRESS
L   = LUGGER,P.,1978,AP.J.221,745
M   = MELNICK,J.,SARGENT,W.,1977,AP.J.,215,401
MA = MACCAGNI,D.,TARENGHI,M.,COOKE,B.A.,MACCACARO,T.,PYE,J.P.,RICKETTS,M.J.,CHINCARINI,G.,1978,ASTRON.ASTROPHYS.,62,127
MQ = MELNICK,J.,QUINTANA,H.,1975,AP.J.,198,L97
MP = MCHARDY,J. AND PYE,J IAU CIRCULAR 3587 1981
MS = SCHMIDT,M.,1968,AP.J.,151,393
N   = NOONAN,T.,1973,A.S.,78,26
OKP = OSTERBROK,D.E.,KOSKI,A.T.,PHILLIPS,M.M.,1976,AP.J.,206,898
S   = SPINRAD,H.,1977,PUB.A.S.P.,89,116
SC = SCHWARTZ,D.,SCHWARZ,J,TUCKER,W.,1980,AP.JLETT. 238,L59
V   = VIDAL,N.V.,1975,PUBL.ASTRON.SOC.PACIFIC,87,625
V1 = WEEDMAN,D.W.,1977,ANN.REV.ASTRON.ASTROPHYS.,15,69
V2 = WEEDMAN,D.W.,1978,MON.NOT.R.ASTR.SOC.,184,11P
V3 = WEEDMAN,D.W.,1979,PROC.IAU GENERAL ASSEMBLY,MONTREAL
WF = WEST,R.M.,FRANDSEN,S.,1980,ESO SCIENT. PREPRINT N.110.

(9) : CONVERSION FACTOR (1.E-11 ERGS/CM2 SEC PER R15 COUNTS/SEC)

(10) : 1ST SCAN LUMINOSITY (1.E44 ERGS/SEC)

(11) : 2ND SCAN LUMINOSITY (1.E44 ERGS/SEC)

(12) : NOTES
1.IPC DETECTION BUT NOT IDENTIFIED AT PRESENT
2.MULTIPLE CLUSTER FORMAN ET AL 1981
3.MULTIPLE CLUSTERS PERRENOD AND HENRY 1981

TABLE 2

HIGH LATITUDE (B> 20 DEG) X-RAY SOURCES EXCLUDED FROM LOG N-LOG S ANALYSIS

Source					Identification	Ref
2A0039+41	1.95	.22	1.47	.37	GALAXY(M31)	V1
H0123+075	1.62	.26	.73	.29	TRANSIENT(HD8357)	M1,G2
2A0311-22	2.64	.22	2.23	.28	STAR	G1
H0328+05	<.85		2.92	.27	STAR	D1
4U0336+01	1.27	.24	1.41	.26	STAR (HR1099)	W1
2S0512-39	6.56	.21	5.64	.25	GLOB CLUSTER(NGC1851)	B1
2A0526-32	1.99	.16	2.55	.20	STAR	C1
H0751+22	1.36	.21	<.6		STAR(U GEM)	S3
2A1052+60	1.34	.21	<.8		STAR(BD 61+1211)	S1
2A1249-28	4.41	.28	5.51	.33	STAR (EX HYA)	S1
3U1616-15	>500.		>500.		SC0X-1(V818 SCO)	B1
3U1655+35	80.8	.43	3.47	.20	HER X-1(HZ HER)	B1
2A1704+24	<.8		2.46	.21	STAR	G4
2A1815+50	4.11	.12	3.98	.14	STAR(AM HER)	S4
H2215-08	1.50	.23	1.20	.40	STAR(WOLF 156127)	T1,S2
4U2127+14	5.32	.22	4.97	.35	GLOB CLUSTER(NGC 7078)	B1
H2252-035	2.36	.25	2.43	.20	STAR	G3

SOURCES IN AND NEAR THE LMC AND SMC HAVE BEEN OMITTED
FROM THIS TABLE AND FROM TABLE 1.THE EXPERIMENT
HAS DETECTED FLUX FROM SMX X-1,2,3 LMC X-1,2,3,4,5
AND THE LMC TRANSIENT SOURCE 0535-668

REFERENCES:
B1=BRADT,DOXSEY,JERNIGAN 1979
C1=CHRALES,THORSTENSEN,BOWYER,MIDDLEDITCH 1979
D1=DOXSEY,MCCLINTOCK,PETRO,REMILLARD,SCHWARTZ
G1=GRIFFITHS,WARD,BLADES,WILSON 1979
G2=GARCIA,BALIUNAS,CONROY,JOHNSTON,RALPH,ROBERTS,SCHWARTZ,TONRY 1980
G3=GRIFFITHS,LAMB,WARD,WILSON,CHARLES,THROSTENSEN,MCHARDY,LAWRENCE 1980
G4=GARCIA,CONROY,DOXSEY,GRIFFITHS,JOHNSTON,RALPH,ROBERTS,SCHWARTZ 1980
M1=MARSHALL,BOLDT,DOXSEY,MUSHOTZKY,PRAVDO,ROTHSCHILD,SERLEMITSOS 1979
S1=SCHWARTZ,BRADT,BRIEL,DOXSEY,FABBIANO,GRIFFITHS,JOHNSTON,MARGON 1979
S2=SCHWARTZ 1980 (PRIVATE COMMUNICATION)
S3=SWANK,BOLDT,HOLT,ROTHSCHILD,SERLEMITSOS 1978
S4=SWANK,LAMPTON,BOLDT,SERLEMITSOS 1977
T1=TSIKOUDI,SWANK 1980
V1=VAN SPEYBROECK,EPSTEIN,FORMAN,GIACCONI,JONES,LILLER,SMARR 1979
W1=WHITE,SANFORD,WEILER 1978

REFERENCES

Avni, Y., Bahcall, J.N. 1980, Ap. J. 235, 694.

Bahcall, N. 1979, Ap. J. 232, 639.

Birnbaum, Z.W., Tingey, F.M. 1951, Ann. Math. Stat 22, 592.

Boldt, E. 1980, Invited Talk at AAS Meeting, NASA TM 80659.

Bradt, H., Doxsey, R.E., and Jernigan, J.G. 1979, Advances in Space
Exploration.

Charles, P. Thorstensen, J., Bowyer, S., and Middleditch, J.1979, Ap. J.
(Letters) 231, L131.

Crawford, D.E., Jauncy, D.L., Murdoch, H.S. 1970, Ap. J. 162, 405.

DeVaucouleurs, G. 1958, A.J. 63, 253.

DeVaucouleurs, G., DeVaucouleurs, A. and Corwin, H. 1976, Second Reference
Catalog of Bright Galaxies, Univ. of Texas Press.

DeZotti, G. 1980, preprint.

Doxsey, R., McClintock, J., Petro, L., Remillard, R., and Schwartz, D. 1981
B.A.A.S. 13, 559.

Elvis, M., Maccacaro, T., Wilson, A., Ward, M., Penston, M., Fosbury, R.,
Perola, G. 1978, MNRAS 183, 129.

Fabian, A.C. and Rees, M.J. 1978, MNRAS 185, 109.

Forman, W., Bechtold, J., Blair, W., Giacconi, R., Van Speybroeck, L. and
Jones, C. 1981, Ap. J. (Letters) 243, L133.

Garcia, M., Baliunas, S.L., Conroy, M., Johnston, M.D., Ralph, E., Roberts,
W., Schwartz, D.A., and Tonry, J. 1980, Ap. J. (Letters) 240, L107.

Garcia, M., Conroy, M., Doxsey, R., Griffiths, R.E., Johnston, M., Ralph, E.,
Roberts,W., and Schwartz, D.A. 1980, BAAS 12, 527.

Giacconi, R., Bechtold, J., Branduaradi, G., Forman, W., Henry, J.P., Jones,
C., Kellogg, E., van der Laan, H., Liller, W., Marshall, H., Murray,

S.S., Pye, J., Schreier, E., Sargent, W.G.W., Seward, F., and Tananbaum, H. 1979, Ap. J. (Letters) 234, L1.

Griffiths, R.E., Ward, M.J., Blades, J.C., Wilson, A.S. 1979, Ap. J. 232, L27.

Griffiths, R.E., Lamb, D.Q., Ward, M.J., Wilson, A.J., Charles, P.A., Thorstensen, J., McHardy, I.M. and Lawrence, A. 1980, MNRAS 193, 25p.

Holt, S.S. 1980, invited talk at Cambridge HEAD meeting, NASA TM 82010.

Huchra, J.P. and Sargent, W.L.W. 1973, Ap. J. 186, 433.

Huchra, J.P. 1977, Ap. J. Suppl. 35, 171.

Huchra, J.P. 1980, private communication.

Kriss, G.A., Canizares, C.R., and Ricker, G.R. 1980, Ap. J. 242, 492.

Lightman, A., Hertz, P., and Grindlay, J.E. 1980, Ap. J. 241, 367.

Marshall, F.E., Boldt, E.A., Holt, S.S., Mushotzky, R.F., Pravdo, S.H., Rothschild, R.E., and Serlemitsos, P.J. 1979, Ap. J. (Suppl) 40, 657.

Marshall, F.E., Boldt, E.A., Holt, S.S., Miller, R., Mushotzky, R.F., Rose, L.A., Rothschild, R., and Serlemitsos, P.J. 1980, Ap. J. 235, 4.

McHardy, I. 1978, MNRAS 182, 760.

McKee, J., Mushotzky, R., Boldt, E., Holt, S., Marshall, F.E., Pravdo, S., and Serlemitsos, P. 1980, Ap. J. 242, 843.

Murdoch, H.S., Crawford, D.F., and Jauncey, D.L. 1973, Ap. J. 183, 1.

Mushotzky, R.F. 1979, Proceedings of the Erice Symposium on X-Ray Astronomy, eds. R. Giacconi and G. Setti, p. 171.

Mushotzky, R., Marshall, F.E., Boldt, E., Holt, S., and Serlemitsos, P. 1980, Ap. J. 235, 36.

Perrenod, S. and Henry, J.P. 1981, preprint.

Pye, J.P. and Warwick, R.S. 1979, MNRAS 187, 905.

Rothschild, R., Boldt, E., Holt, S., Serlemitsos, P., Garmire, G., Agrawal, P., Riegler, G., Bowyer, S., and Lampton, M. 1979, Space Science

Instrumentation 4, 265.

Schwartz, D.A. 1978, Ap. J. 222, 8.

Schwartz, D.A., Bradt, H., Briel, V., Doxsey,R.E., Fabbiano, G., Griffiths,

R.E., Johnston, M.D., Margon, B. 1979, Ap. J. 84, 1560.

Schwartz, D.A., 1979 in (COSPAR) X-Ray Astronomy, W.A. Baity and L.E. Peterson

(eds), Pergamon Press, Oxford and New York, p.453.

Schwartz, D.A. 1980, private communication.

Swank, J., Boldt, E.A., Holt, S.S., Rothschild, R.E., and Serlemitsos, P.J.

1978, Ap. J. (Letters) 226, L133.

Swank, J., Lampton, M., Boldt, E., Holt, S., and Serlemitsos, P. 1977, Ap. J.

(Letters) 216, L71.

Tananbaum, H., Peters, G., Forman, W., Giacconi, R., Jones, C., and Avni, Y.

1978, Ap. J. 223, 74.

Tsikoudi, V. and Swank, J. 1981, in preparation.

Van Speybroeck, L, Epstein, A., Forman, W., Giacconi, R., Jones, C., Liller,

W., and Smarr, L. 1979, Ap. J. 234, L45.

Warwick, R.S. and Pye, J.P. 1978, MNRAS 183, 169.

Weedman, D. 1979, Invited Talk at Montreal IAU General Assembly.

Weinberg, S. 1972, Gravitation and Cosmology

West, R.M., and Frandsen, S. 1980, ESO Scientific Preprint, No. 110.

White, N.E., Sanford, P.W., and Weiler, E.J. 1978, Nature 274, 569.

Worrall, D., Boldt, E., Holt,S., Mushotzky, R., and Serlemitsos, P. 1981, Ap.

J. 243, 53.

FIGURE CAPTIONS

Figure 1. The completeness level of the present survey vs ecliptic latitude. The diamonds are for the first pass and the crosses for the second pass. The lower histogram is the sky fraction in each ecliptic latitude bin (right hand scale). The centre of the diamonds and crosses is 5 times the mean error for a source located in that ecliptic latitude bin and the size of the error bar is the standard deviation of this error. Since we truncate at 1.25 R15 counts all of our sources at ecliptic latitude greater than 30° lie well above the 5σ level. We estimate that residual incompleteness of sources at levels less than 1.4 cts is less than 3 sources and zero sources greater than this limit.

Figure 2. The error boxes for H0328+025 and H0917-074. The inner and outer boxes are the 90% confidence boxes as described in Marshall et al. 1979. The inner box assumes that the source was roughly constant during our period of observation.

Figure 3. The distribution of the non-galactic sources detected in this survey in supergalactic coordinates.

Figure 4. The probability distributions for κ and α. The top panel shows the AML probability vs α in the first pass data, the middle panel shows the AML probability vs α in the second pass. The bottom panel shows the 68 and 95% joint probability contour for κ and α for the first pass data. The + marks the best fit.

Figure 5. The differential log N - log S distribution for our sample. The best fit is indicated. The highest flux point is indicated by a dashed cross because its upper flux bound is not well defined. (1st pass data)

Figure 6. The AML Kolomogorov-Smirnov test distribution for an $\alpha = 2.5$ model. The 50 and 95% probability bounds are indicated. (1st pass data)

Figure 7. The ratio of the number of observed sources N_{obs} to the number of expected sources for $\alpha = 2.5$ log N - log S law. (1st pass data)

Figure 8a. The cluster of galaxies differential luminosity function for the first pass data.

   8b. The same information for the second pass data. The best fit
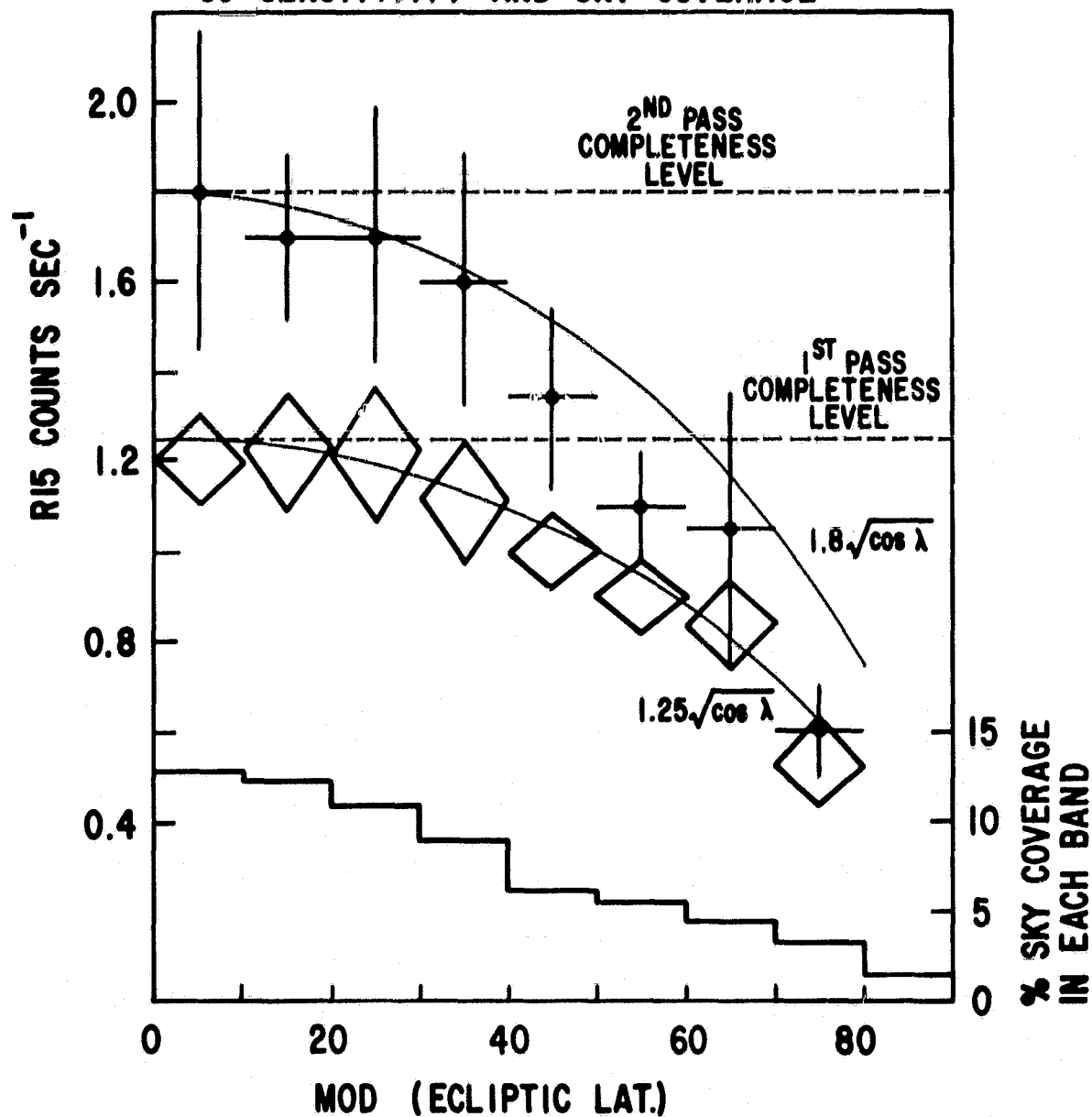   power   law models are indicated on both panels.

Figure 9. the AML probability vs. γ the slope of the power law differential luminosity function for clusters of galaxies for the first and second passes including and excluding the Virgo cluster.
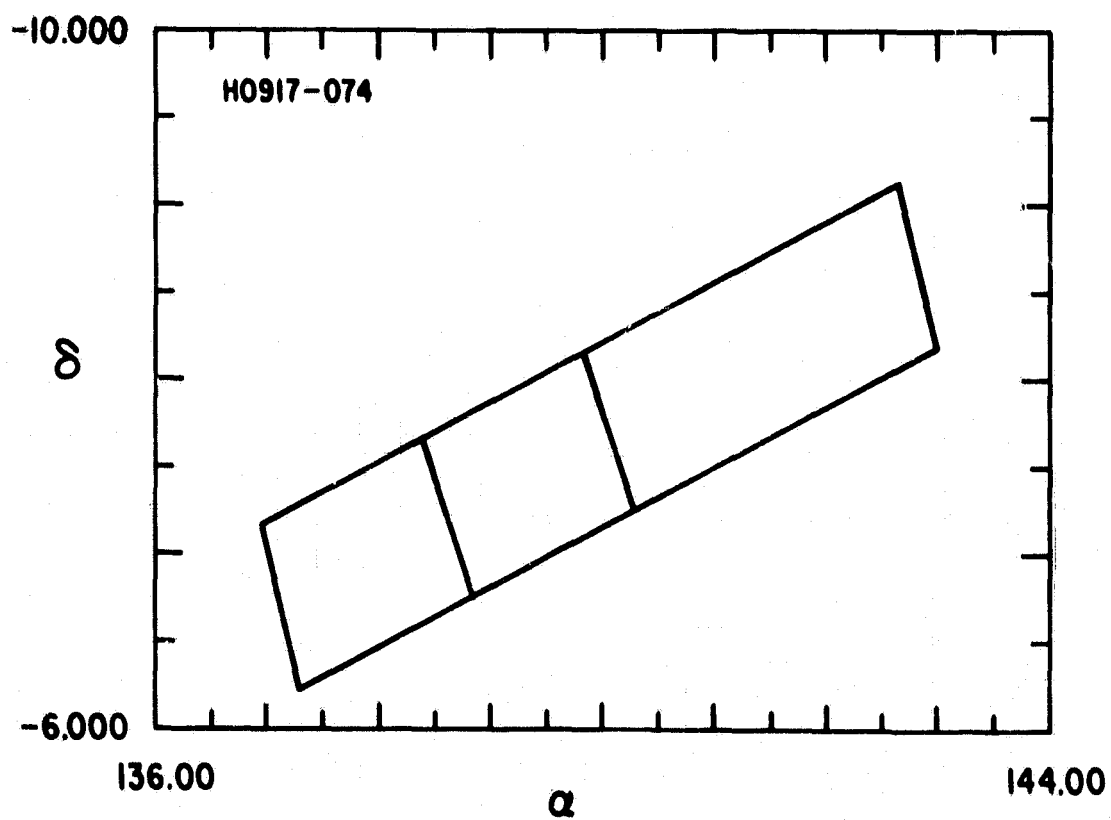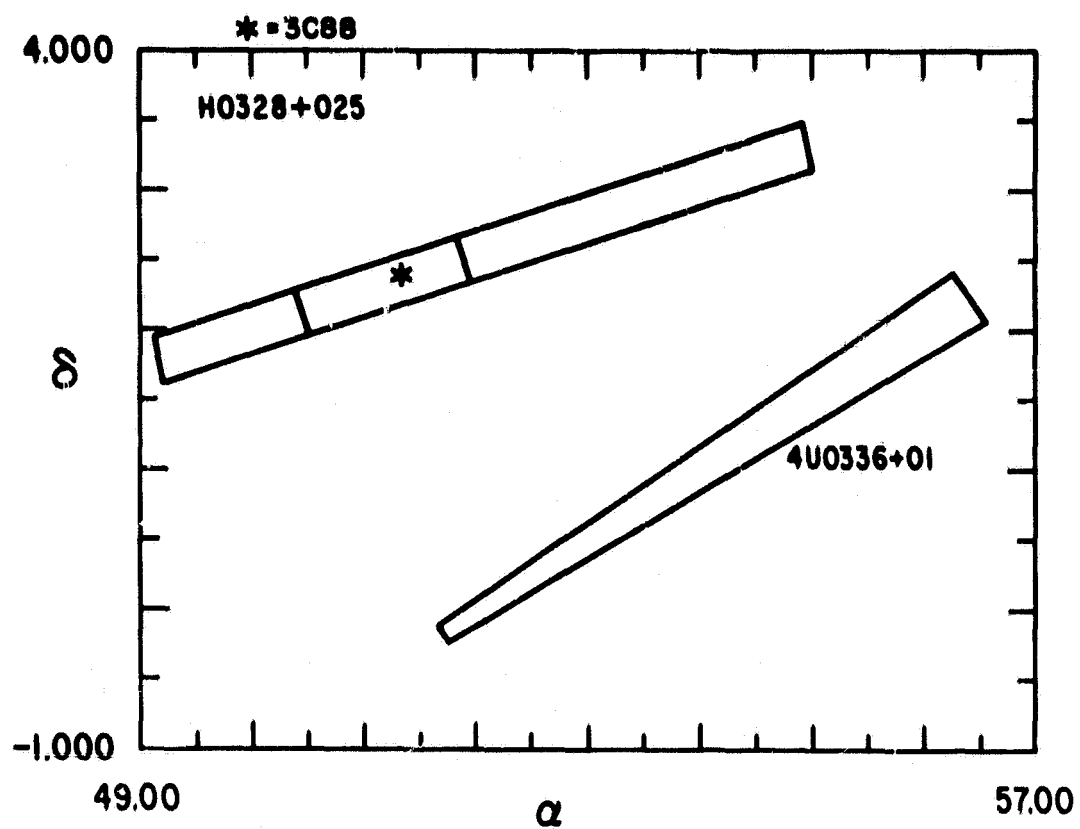
Figure 10. Same as Figure 9 but for the exponential luminosity function..

Figure 11. The Seyfert galaxy luminosity function for the first pass data. The best fit power law differential model is indicated. The insert shows the AML probability vs. γ the slope of the luminosity function.
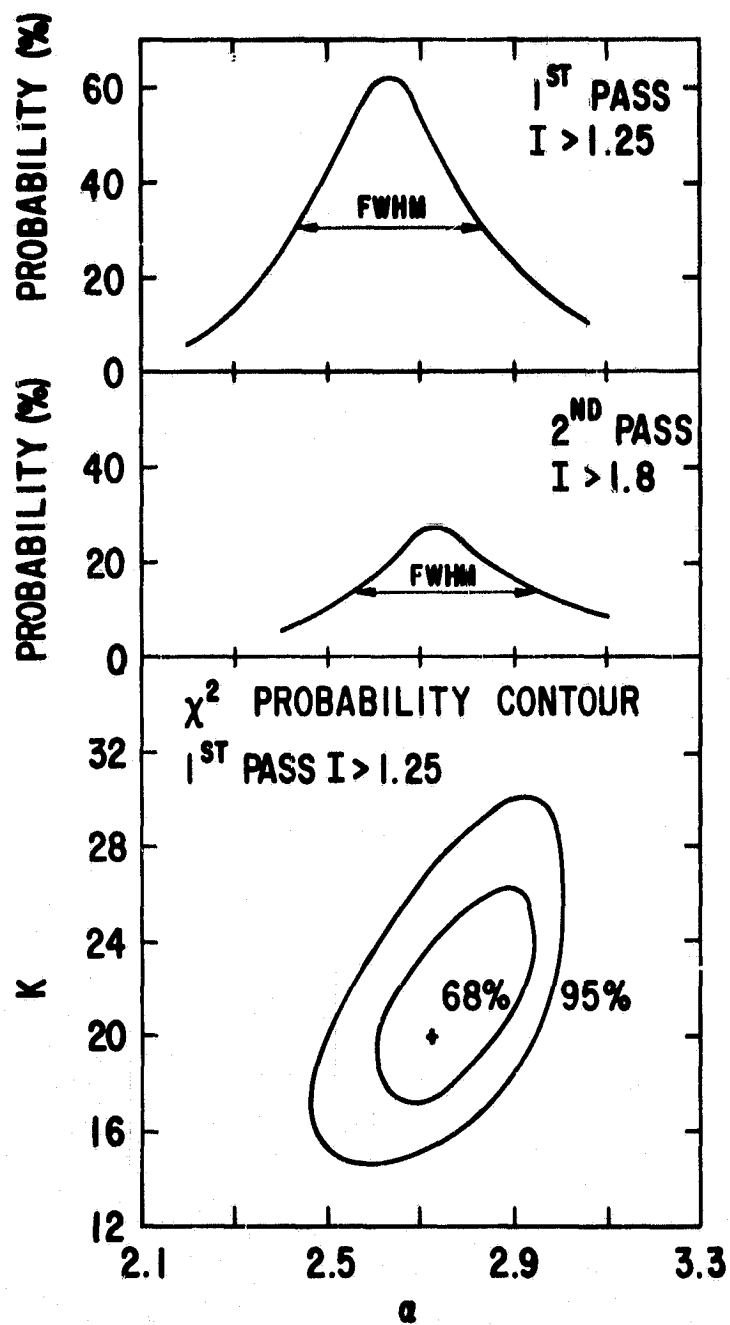
5σ SENSITIVITY AND SKY COVERAGE

4.000
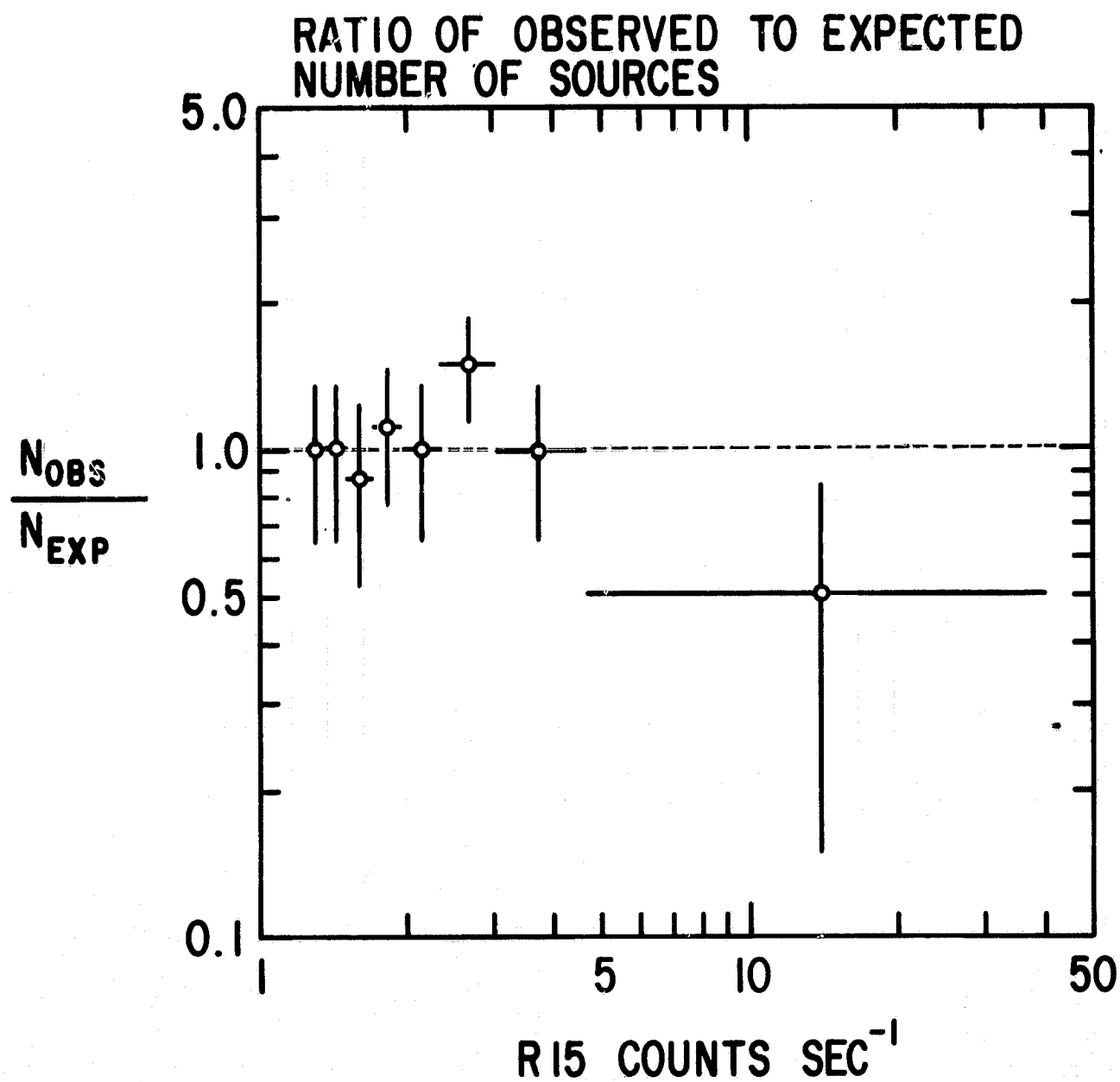
* = 3C88

H0328+025

δ

*

4U0336+01

-1.000

49.00 α 57.00

-10.000

H0917-074

δ

-6.000

136.00 α 144.00

SUPERGALACTIC COORDINATES

S > 1.25 R15 COUNTS SEC^{-1}

* UNIDENTIFIED SOURCES
● CLUSTERS
○ GALAXIES
□ Z ≤ 0.01

RATIO OF OBSERVED TO EXPECTED
NUMBER OF SOURCES

$$\frac{N_{OBS}}{N_{EXP}}$$

R15 COUNTS SEC^{-1}

AML−KS TEST FOR EUCLIDEAN MODEL:
$\alpha = 2.5$ (1ST PASS − S ≥ 1.25 R15 COUNTS SEC^{-1})

log N ~ log S DISTRIBUTION

HEAO-I A2

$20\ S^{-2.72}$

CLUSTERS OF GALAXIES LUMINOSITY FUNCTION

$I > 1.8$ R15 COUNTS/SEC

$N(L_{44}) = 3.8 \times 10^{-7} L_{44}^{-2.15}$

SECOND SCAN

$I > 1.25$ R15 COUNTS/SEC

$N(L_{44}) = 3.3 \times 10^{-7} L_{44}^{-2.15}$

FIRST SCAN

L_{44} (10^{44} ERGS/SECOND)

$N(L_{44})$ MpC^{-3} (10^{44} ERGS/SECOND)$^{-1}$
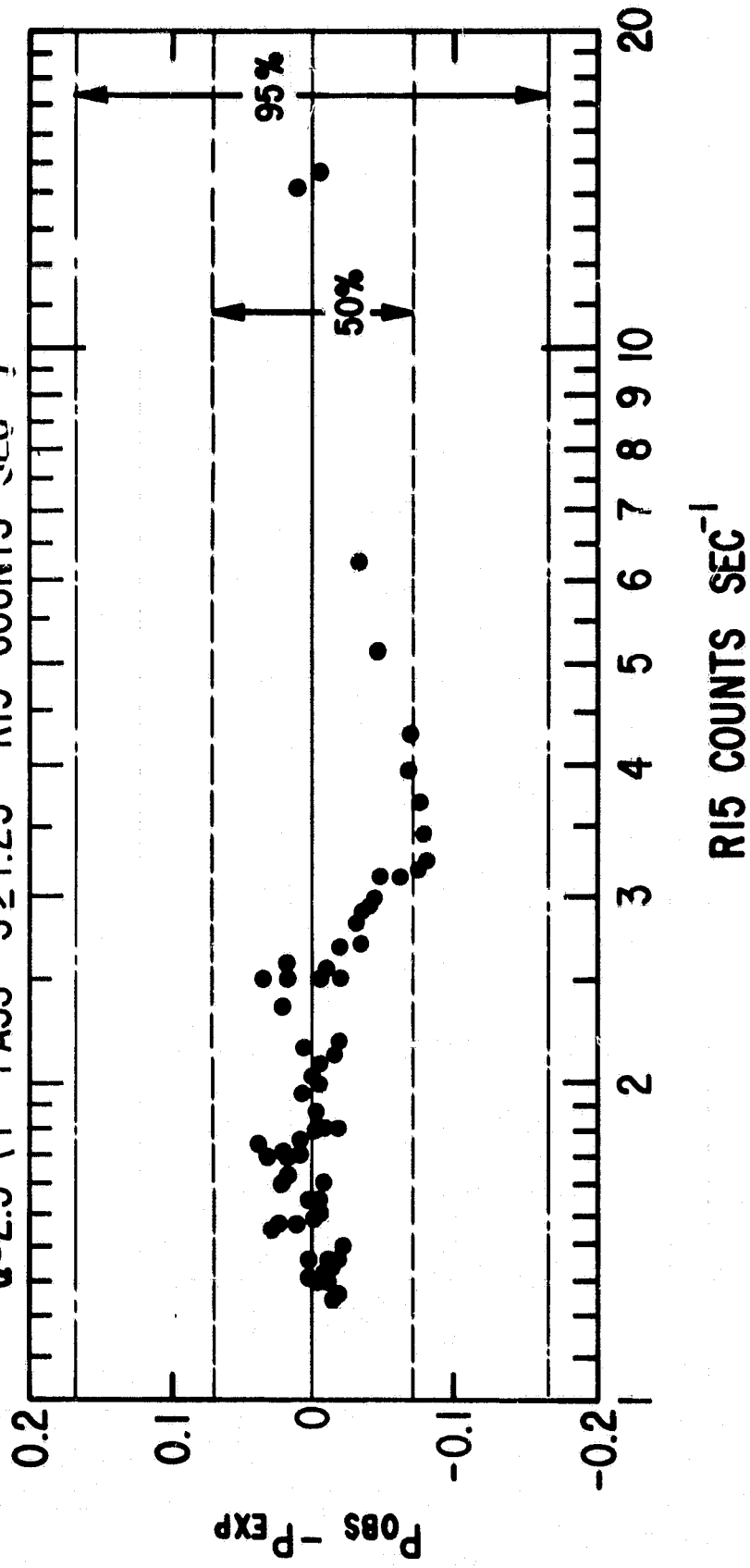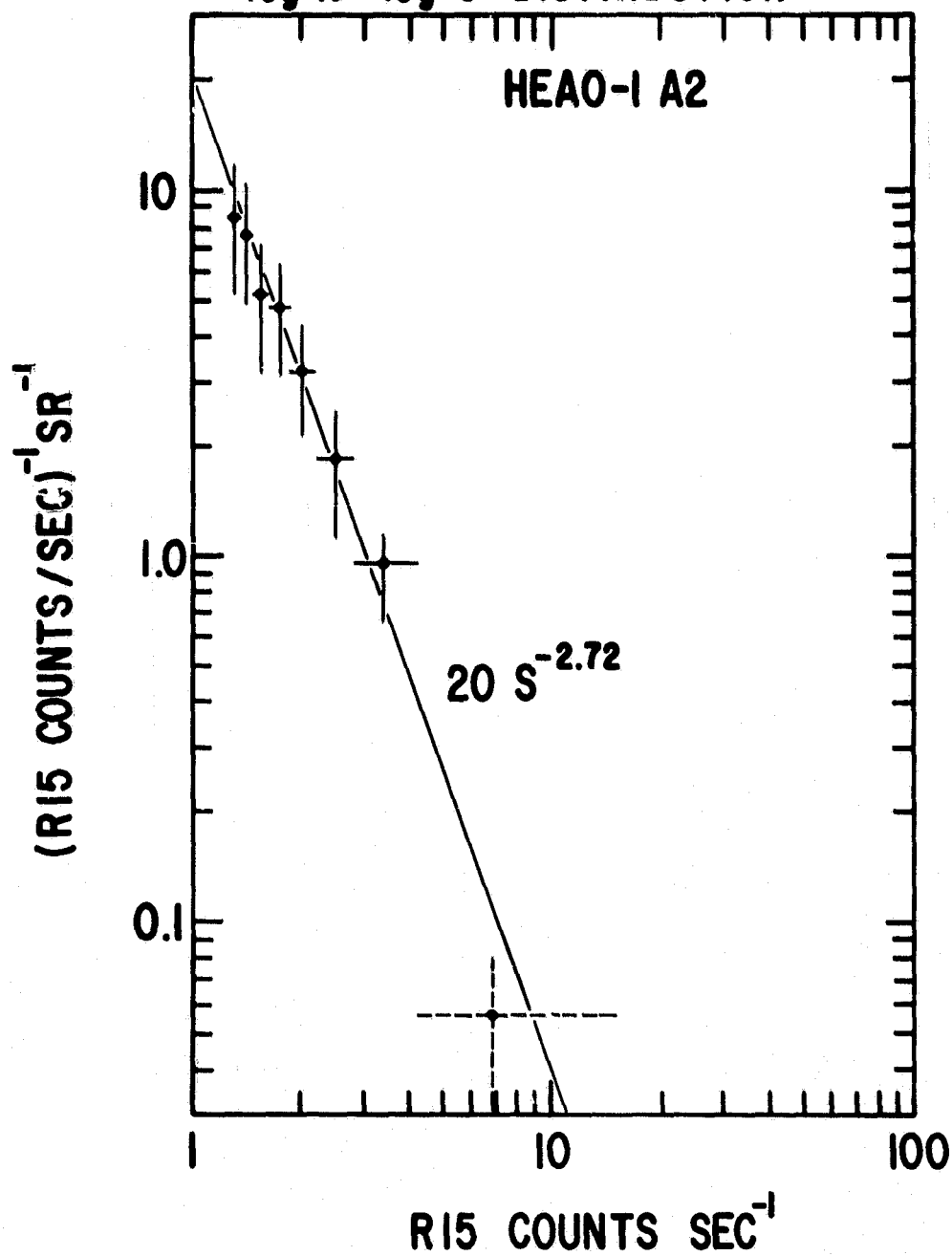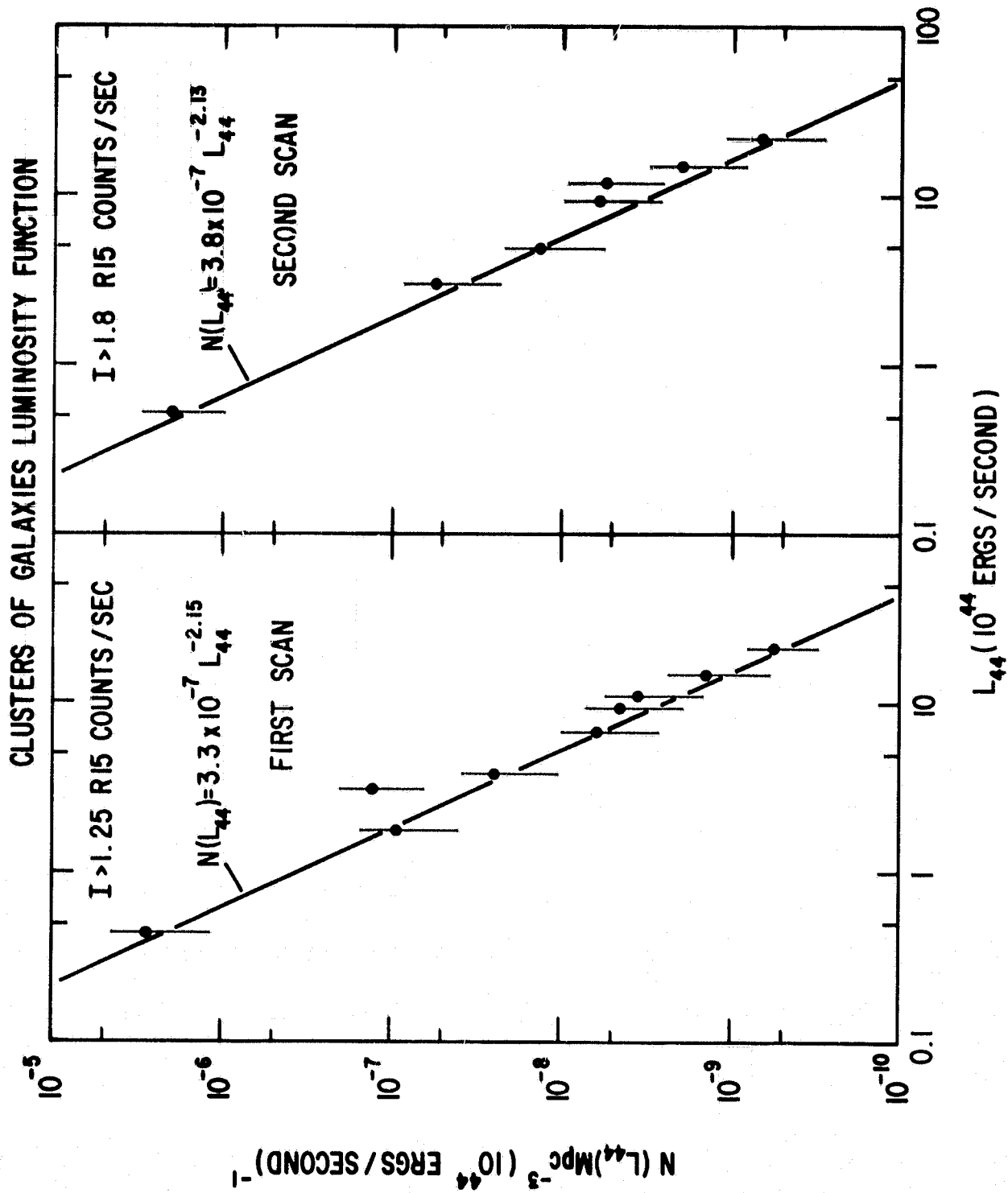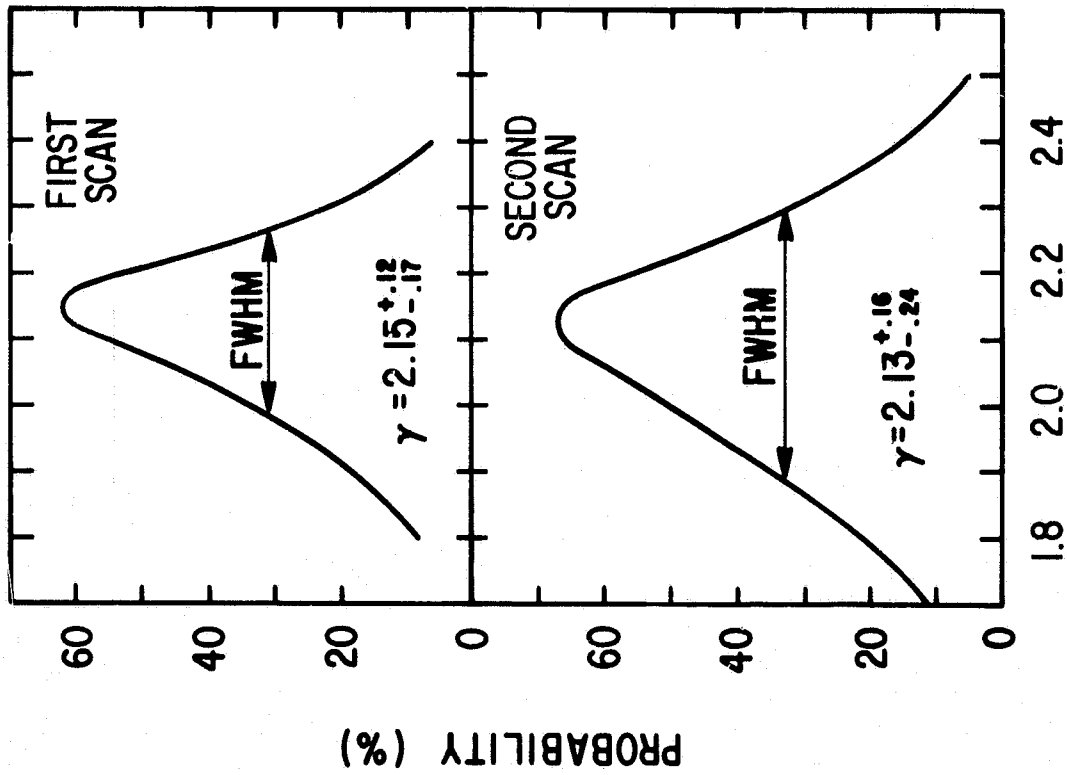
POWER LAW MODEL (WITHOUT VIRGO)

FIRST SCAN

FWHM

$\gamma = 2.03 \pm .18$

SECOND SCAN

FWHM

$\gamma = 2.07^{+.20}_{-.25}$

POWER LAW MODEL (WITH VIRGO)

FIRST SCAN

FWHM

$\gamma = 2.15^{+.12}_{-.17}$

SECOND SCAN

FWHM

$\gamma = 2.13^{+.16}_{-.24}$

PROBABILITY (%)

γ

EXPONENTIAL LUMINOSITY FUNCTION
(WITHOUT VIRGO)

FIRST SCAN

SECOND SCAN

EXPONENTIAL LUMINOSITY FUNCTION
(WITH VIRGO)

FIRST SCAN

SECOND SCAN

PROBABILITY (%)

$L_{0_{44}}$

SEYFERT GALAXIES LUMINOSITY FUNCTION

$N(L_{44}) = 2.68 \times 10^{-7} L_{44}^{-2.75}$

FIRST SCAN
I > 1.25 R15 COUNTS / S

ACTIVE
GALAXIES
FIRST
SCAN

FWHM

$\gamma = 2.75 \pm .15$